

# A large deletion spanning *PITX2* and *PANCR* in a Chinese family with Axenfeld-Rieger syndrome

Yayun Qin,<sup>1</sup> Pang Gao,<sup>1</sup> Shanshan Yu,<sup>1</sup> Jingzhen Li,<sup>1</sup> Yuwen Huang,<sup>1</sup> Danna Jia,<sup>1</sup> Zhaohui Tang,<sup>1</sup> Pengcheng Li,<sup>2</sup> Fei Liu,<sup>1</sup> Mugen Liu<sup>1</sup>

<sup>1</sup>Key Laboratory of Molecular Biophysics of Ministry of Education, College of Life Science and Technology, Huazhong University of Science and Technology, Wuhan, P.R. China; <sup>2</sup>Department of Ophthalmology, Union Hospital, Tongji Medical College, Huazhong University of Science and Technology, Wuhan, P.R. China

**Purpose:** To identify the genetic cause in a four-generation Chinese family with Axenfeld-Rieger syndrome (ARS).

**Methods:** The family members received clinical examinations of the eye, tooth, periumbilical skin, and heart. Sanger sequencing and whole-exome sequencing (WES) were performed to screen potential mutations. The genomic deletion region around the *PITX2* gene was estimated from single nucleotide polymorphism (SNP) data from WES and then confirmed with “quantitative PCR (qPCR) using a set of primers. The DNA breakpoint was further identified with long-range PCR and Sanger sequencing.

**Results:** Symptoms including anterior segment dysplasia of the eye (iris dysplasia, multiple pupils, and posterior embryotoxon), dental dysplasia, and periumbilical skin redundancy were present in all of the affected individuals. Three of them had glaucoma. Corneal abnormalities (inferior sclerocornea, corneal endothelial dystrophy, and central corneal scar) were seen in most of the affected individuals. Cataract, limited eye movement, electrocardiographic abnormalities, intellectual disability, and recurrent miscarriages were observed in some of the affected individuals. No mutations in the coding and exon-intron adjacent regions of the *PITX2* and *FOXC1* genes were identified with Sanger sequencing. According to the SNP data from WES, we suspected that there might be a deletion region (at most 1.6 Mb) around the *PITX2* gene. With the use of qPCR and long-range PCR, we identified a 53,840 bp deletion (chr4: 111,535,454–111,588,933) spanning *PITX2* and *PANCR*. The genomic deletion cosegregated with the major ARS symptoms observed in the family members.

**Conclusions:** With the help of WES, qPCR, and long-range PCR, we identified a genomic deletion encompassing *PITX2* and the adjacent noncoding gene *PANCR* in a Chinese family with ARS. The clinical features of the affected individuals are reported. This work may broaden understanding of the phenotypic and mutational spectrums related to ARS.

Axenfeld-Rieger syndrome (ARS) is a rare disease primarily characterized by abnormal development of the anterior segment of the eye, such as iris hypoplasia, corectopia, polycoria, posterior embryotoxon, and corneal abnormalities [1-3]. Around 50% of patients with ARS develop glaucoma, which leads to blindness without appropriate intervention. Extraocular symptoms, such as dental anomalies, redundant periumbilical skin, craniofacial abnormalities, heart defects, hearing loss, and so on, can also be observed in all or some of the patients with ARS [1,2].

ARS is inherited in an autosomal dominant manner. Mutations in the major pathogenic genes *PITX2* (OMIM 601542) and *FOXC1* (OMIM 601090) account for about 40–70% of the patients with ARS [2,4]. In addition to the common intragenic mutations (missense, nonsense, splicing, and small deletion/insertion), large deletions affecting the entire or part of the coding and upstream regulatory regions

of *PITX2* and *FOXC1* have also been reported [5-7]. Another two genes (*CYP11B1*-Gene ID: 1545, OMIM: 601771 [8] and *PRDM5*-Gene ID: 11107, OMIM: 614161 [9]) and one locus (13q14 [10]) have also been implicated with ARS. However, the underlying genetic causes in at least 30% of patients with ARS remain unclear.

Genotype–phenotype studies indicate that mutations in *PITX2* are more commonly associated with additional systemic symptoms such as dental, umbilical, and craniofacial abnormalities. Meanwhile, patients with mutations in *FOXC1* often show ocular symptoms alone or combined with heart and hearing defects [4,6,11]. However, recent studies also reported that mutations in *PITX2* can result in dental anomalies [12] and heart diseases [13-16] without the classical symptoms of ARS.

We report a four-generation family with ARS from Hubei province, China. The clinical features of the affected individuals are summarized. With the help of whole-exome sequencing (WES), quantitative PCR (qPCR), and long-range PCR, a genomic deletion spanning *PITX2* and *PANCR* (Gene ID: 110231149, OMIM: 617286) was identified.

Correspondence to: Fei Liu, Key Laboratory of Molecular Biophysics of Ministry of Education, College of Life Science and Technology, Huazhong University of Science and Technology, Wuhan 430074, P.R. China; liufei05@hust.edu.cn

## METHODS

*Participant recruitment and clinical examinations:* Eleven patients from a four-generation non-consanguineous family were recruited from Yangxin, Hubei, China, and were investigated in the study. The gender, age, and health condition for each patient were shown in Table 1. Written informed consent was signed by all participants or their statutory guardians. The study was approved by the Ethics Committee of Huazhong University of Science and Technology. The authors declared that this study adhered to the ARVO statement on human subjects. Clinical examinations of the participants were performed at the Union Hospital (affiliated with Tongji Medical College, Huazhong University of Science and Technology) and the Yangxin People's Hospital. Affected individual IV:1 died of unknown causes at the age of 5. He had undergone a clinical examination when he was alive. Peripheral blood samples (1-3 ml) were collected from the anterior elbow vein by clinicians for each participant and stored in EDTA blood collection tubes at 4 °C. Genomic DNA was prepared using the TIANamp Blood DNA Kit DP348 (Tiangen Biotech, Beijing, China) as described previously [17].

*Mutation screening with Sanger sequencing and whole-exome sequencing:* The coding exons and the exon-intron boundaries of *PITX2a* (NM\_001204399), *PITX2b* (NM\_001204397), *PITX2c* (NM\_000325), and *FOXC1* (NM\_001453) were amplified with PCR using primers listed in Appendix 1. The following PCR conditions were used: predegeneration at 95 °C for 5 min; 35 cycles of denaturation at 95 °C for 30 s, annealing at 60 °C for 30 s and extension at 72 °C for 30–60 s; a final extension at 72 °C for 10 min. A total of 50 ng of genomic DNA was added as the template in a 30 µl reaction volume. The PCR products were examined with agarose gel electrophoresis and subjected to Sanger sequencing as described previously [18,19].

WES was performed using the xGen Exome Research Panel v1 (Integrated DNA Technologies, Coralville, IA) and the HiSeq 2500 platform (Illumina, San Diego, CA) at Nextomics Biosciences Corporation (Wuhan, China). Bioinformatic analysis was performed as described previously [20]. Briefly, the raw sequences were mapped to the human reference genome (hg19) with Burrows-Wheeler Aligner (BWA) [21]. Variants were detected with genome analysis toolkit (GATK), using standard hard filtering parameters according to GATK Best Practices recommendations [22], and then annotated with wANNOVAR [23]. After intergenic, intronic, untranslated region (UTR), and synonymous variants were removed, variants with a minor allele frequency (MAF) of

>0.005 were further filtered out using the 1000 Genomes Project and the gnomAD exome database.

*qPCR and long-range PCR:* A set of primers (Appendix 2) spanning the *PITX2* gene were designed to detect whether the region is haploid or diploid with qPCR using the AceQ™ qPCR SYBR Green Master Mix (Vazyme Biotech, Nanjing, China) and the StepOnePlus™ real-time PCR System (Applied Biosystems, Foster City, CA). The following qPCR conditions were used: predegeneration at 95 °C for 5 min, followed by 40 cycles of denaturation at 95 °C for 10 s, annealing and extension at 60 °C for 30 s in a 20 µl reaction volume with 50 ng of genomic DNA as the template. To amplify the region containing the DNA breakpoint, long-range PCR was performed using -26.4k-F/+4.5k-R primers and PrimeSTAR GXL DNA Polymerase (Takara Biomedical Technology, Beijing, China) under the default condition suggested by the product manual. The exact sequence was further determined with Sanger sequencing.

## RESULTS

*Pedigree analysis and clinical manifestations:* Affected individuals were observed in every generation, indicating a dominant inheritance pattern in the family (Figure 1A). The DNA samples from II:2 and IV:1 were unavailable. The clinical findings of the affected individuals are summarized in Table 1. Common symptoms of ARS, such as iris dysplasia, multiple pupils, posterior embryotoxon, dental dysplasia, and periumbilical skin redundancy, were observed in all of the affected individuals. Glaucoma was observed in affected individuals II:3, III:2, III:9 (suspected), and IV:3. Corneal abnormalities (inferior sclerocornea, central corneal scar, reduced endothelial density, and corneal endothelial dystrophy) were seen in most of the affected individuals with the exception of two children (IV:4 and IV:5). Interestingly, affected individual II:10 showed significant decreases in endothelial densities in both eyes (1,675/777 cells/mm<sup>2</sup>, reference value: 2,935±285.0 cells/mm<sup>2</sup> [24]; Figure 1C). Affected individuals III:7 and III:9 also exhibited reduced endothelial density and limited eye movement. Affected individuals II:3, III:2, and IV:2 had cataracts. Affected individuals IV:1 and IV:2 showed developmental retardation and intellectual disability. Finally, affected individual II:10 had also suffered three miscarriages.

*Identification of the genetic cause within the family:* Based on the clinical features and family history, the candidate genes *PITX2* and *FOXC1* were screened directly with Sanger sequencing. No mutations were identified in the coding regions and exon-intron boundaries of either gene. Due to the lack of male to male transmission in the family, we suspected

TABLE 1. THE CLINICAL MANIFESTATIONS OF THE PATIENTS IN THE FAMILY.

Patient	Age	Sex	Iris dysplasia	Multiple pupils	Posterior embryotoxon <sup>a</sup>	Glaucoma <sup>b</sup>	Cataract	IOP <sup>c</sup>	Corneal abnormalities	Limited eye movement	Dental dysplasia	Perium-bilical skin redundancy	ECG abnormalities
II:1	54	M	-	+	+	-	-	13/15	small cornea	-	+	+	N.D.
II:3	52	M	+	-	-	18	+	Tn+1/	central corneal scar	-	+	+	ST-segment deviation
								Tn+1					V2-V5: T-waves inversion I, II, V6: T-waves low-flat
II:10	47	F	+	+	+	-	-	16/15	endothelium dystrophy	-	+	+	N.D.
III:2	36	F	-	+	-	19	+	Tn/ Tn	central corneal scar	-	+	+	N.D.
III:7	30	F	+	-	-	-	-	27/27	reduced endothelial density	+	+	+	N.D.
III:9	27	F	+	-	-	suspected	-	30/31	reduced endothelial density	+	+	+	ST-segment deviation
IV:1 <sup>d</sup>		M	+	N.D.	N.D.	N.D.	N.D.	N.D.	central corneal scar	N.D.	+	+	N.D.
IV:2	18	F	+	-	+	N.D.	+	N.D.	inferior sclerocornea	-	+	+	N.D.
IV:3	17	F	+	-	+	15	-	56/	inferior sclerocornea	-	+	+	arrhythmia

N.D., not determined. <sup>a</sup>, examined under slit lamp. <sup>b</sup>, the number indicate the ages at which glaucoma was found. <sup>c</sup>, II:3 and III:2 underwent anti-glaucoma surgery at the age of about 20. They received IOP measurement (ocular tonometry) at the age of 44 and 28. <sup>d</sup>, IV:1 died of unknown causes at the age of 5.

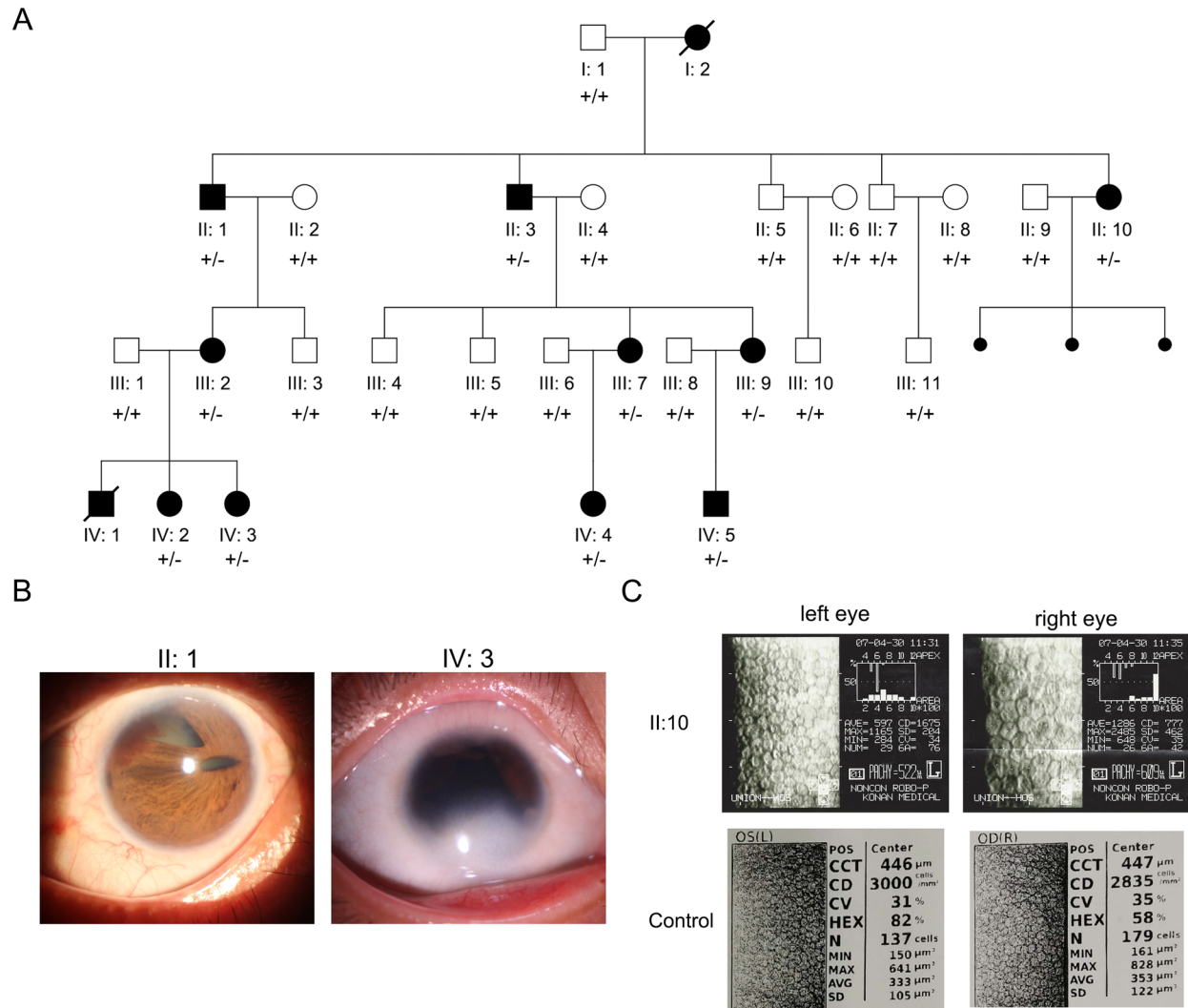


Figure 1. The pedigree and ocular symptoms of the family with ARS. **A:** Family members and their relationships are shown. The affected individuals are labeled with filled symbols. Circle, female; square, male; small filled circle, miscarriage. “+” represents the normal allele, and “-” represents the deletion allele. **B:** Iris dysplasia and multiple pupils are shown for affected individuals II:1 and IV:3. **C:** Specular microscopy examination of affected individual II:10 (upper panel) and an age-matched control (lower panel). Significantly reduced corneal endothelial cell density is shown in both eyes of II:10.

a possibility of X-linked dominant inheritance. Therefore, whole-exome sequencing was performed on affected individual II:3 to ascertain whether there were any variants on the X chromosome responsible for the ARS symptoms within the family. After the intergenic, intronic, UTR, and synonymous variants were removed, 904 variants with a MAF of <0.005 were noted. Thirteen of these variants were located on the X chromosome (Appendix 3). As the affected individual II:3 chosen for WES is male, four homozygous variants including p.S489fs in *ARSF* (Gene ID: 416, OMIM: 300003), p.A224T in *MAGED1* (Gene ID: 9500, OMIM: 300224), p.L57insQQ in *AR* (Gene ID: 367, OMIM: 313700), and p.L933F in *COL4A5*

(Gene ID: 1287, OMIM: 303630) were selected to perform co-segregation analysis. However, none of them cosegregated with the disease in the family.

The possibility of large fragment deletions in *PITX2* was not excluded in the study above, and the ocular and extra-ocular symptoms strongly suggested *PITX2* as the disease-causing gene. Next, we investigated the genotypes of single nucleotide polymorphisms (SNPs) around the *PITX2* gene based on the WES data. We found that in an approximate 1.6 Mb region spanning *ENPEP* (Gene ID: 2028, OMIM: 138297), *PANCR*, *PITX2*, and *C4orf32* (Gene ID: 132720), all of the detected SNPs were homozygous, which increased

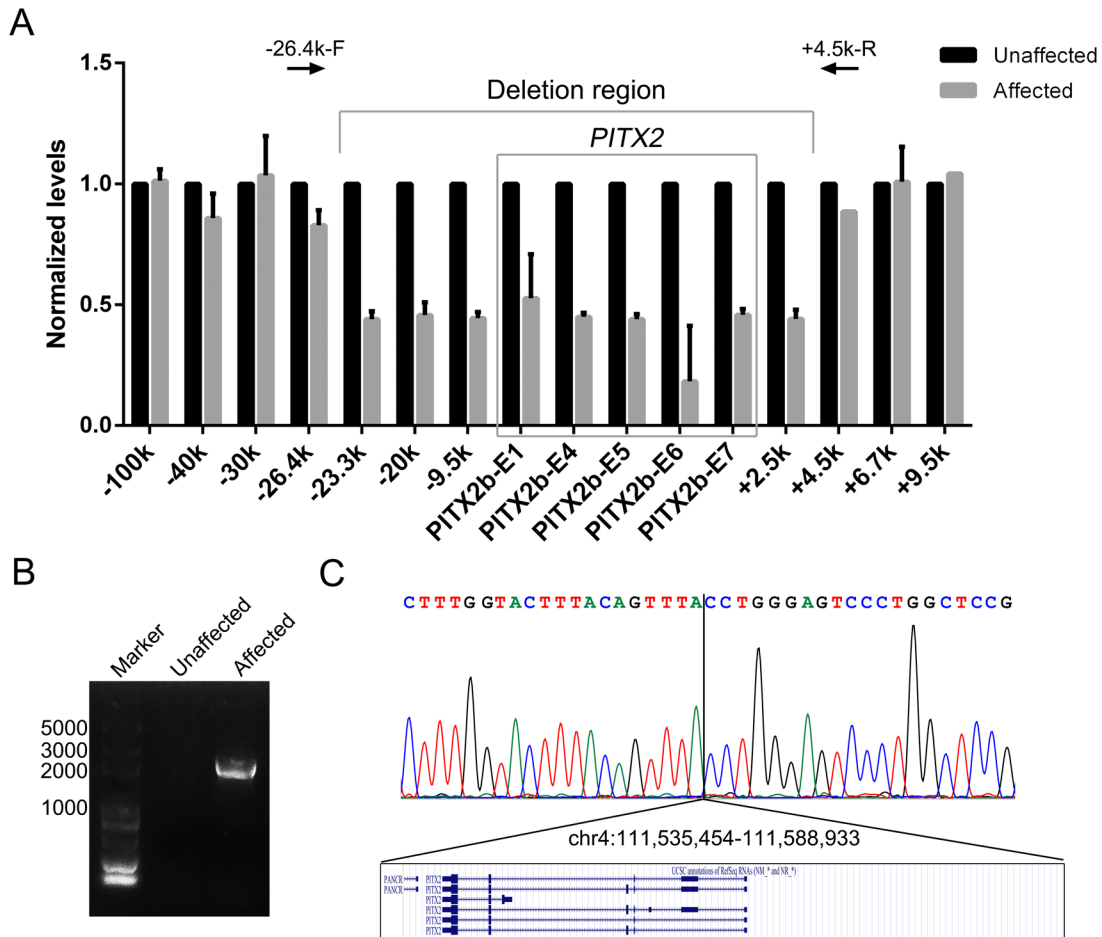


Figure 2. Identification of the large genomic deletion spanning *PITX2* in the family. **A**: Confirming and mapping the deleted region around *PITX2* with quantitative PCR (qPCR). The deletion was positioned between 26.4 kb upstream and 4.5 kb downstream of the *PITX2* gene. **B**: The DNA fragment containing the breakpoint was amplified with long-range PCR using the -26.4k-F/+4.5k-R primers. **C**: The sequencing result of the DNA fragment above shows an approximate 50 kb deletion spanning the first exon of *PANCR* and the entire *PITX2* gene.

the possibility of the haploid status of the whole or part of the *PITX2* gene.

To confirm the deletion and identify the exact DNA breakpoint, we performed qPCR analysis on DNA from individuals III:5 (unaffected) and III:9 (affected) using primers covering the exons and the 5'- and 3'- regions of *PITX2* (Appendix 2). All of the examined exons were haploid in the affected individual (Figure 2A), confirming the deletion of the whole *PITX2* gene. The deletion range was identified by extending the qPCR primers upstream and downstream of *PITX2*. The DNA breakpoint was located between -26.4 kb to -23.3 kb upstream of *PITX2* and +2.5 kb to +4.5 kb downstream of *PITX2*. Using the -26.4k-F/+4.5k-R primer pair, an approximate 2 kb DNA fragment was amplified only in affected individual III:9 (Figure 2B). Sanger sequencing of this fragment uncovered a 53,840 bp deletion (chr4:

111,535,454–111,588,933; Figure 2C), which contained the whole *PITX2* gene and the first exon of the noncoding gene *PANCR*. The deletion exactly cosegregated with the disease in the family, as detected with PCR amplification using the -26.4k-F/+4.5k-R primer pair (Appendix 4).

*Electrocardiographic abnormalities in affected individuals:* Several studies have shown that *PITX2* plays an important role in the development and maintenance of the heart [25-28]. The adjacent lncRNA *PANCR* regulates the expression of *PITX2c*, the cardiac-specific transcript of *PITX2* [29]. In addition, mutations in *PITX2* have been associated with a wide range of heart defects, such as atrial fibrillation [14,16], tetralogy of Fallot [13,30], and congenital atrial septal defects [31]. However, no signs of heart disease were reported by any of the affected family members. To investigate any potential asymptomatic cardiac anomalies, affected (II:3, III:9,



and IV:3) and unaffected (III:5) individuals received color Doppler echocardiography and electrocardiography tests. No obvious changes in the heart structure were observed in affected individuals II:3 and III:9. Affected individual IV:3 showed left ventricular false tendon and arrhythmia. The electrocardiograph of IV:3 also demonstrated the presence of arrhythmia and ST-T abnormalities (Figure 3, Table 1). Furthermore, affected individuals II:3 and III:9 also presented ST-T abnormalities with normal sinus rhythm (Figure 3, Table 1). These changes were not detected in unaffected individual III:5.

## DISCUSSION

*PITX2* encodes a homeobox transcription factor that plays an essential role in the development of many organs [32-34]. Complete deletion of *Pitx2* in mice causes embryonic lethality and multiorgan malformations, including ARS-related

anomalies and heart defects [35,36]. Heterozygous *Pitx2*-null mice show the ocular features of ARS and glaucoma [37], and are susceptible to atrial arrhythmias [28]. Doubtlessly, *PITX2* is important for normal heart function. In this study, individuals with ARS showed no obvious heart structural symptoms or defects. However, the ECG revealed irregularities in cardiac electrophysiology in some of the affected individuals. A patient with ARS with a mutation in *PITX2* was previously diagnosed with Wolf-Parkinson-White (WPW) syndrome [3]. WPW syndrome is a form of heart disease characterized by tachycardia and other changes in ECG. More than half of individuals with WPW syndrome are asymptomatic, but they have a low risk of undergoing cardiac arrest or sudden cardiac death [38]. To a certain extent, the cardiac features of patients examined in this family may belong to the category of WPW syndrome. Nevertheless, compared with the eye, tooth, and periumbilical skin abnormalities, heart defects are rarely reported in patients with mutations in *PITX2*.

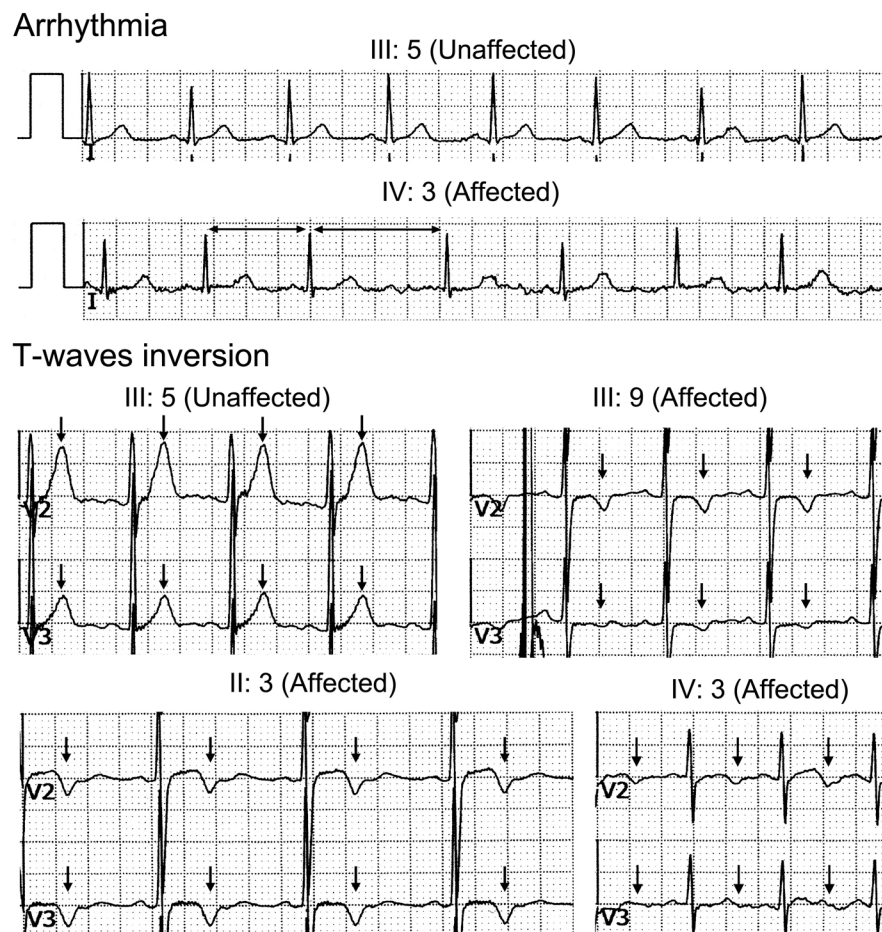


Figure 3. The electrocardiographic abnormalities of the affected individuals in the family. IV:3 shows arrhythmia (indicated by the horizontal arrows). II:3, III:9, and IV:3 show ST-T abnormalities (indicated by arrows).

Other unusual features, such as limited eye movement, corneal abnormalities, cataract, recurrent spontaneous miscarriages, and intellectual disability, were observed in certain patients in the family. *Pitx2* is required for the development and maintenance of extraocular muscles [39], which may explain the presence of limited eye movement in the two patients in this study. Most of the patients (except the two young children) in this family showed corneal abnormalities, which are thought to be infrequent in patients with ARS according to previous reports [1,2]. Developmental retardation and intellectual disability have also been reported in patients with mutations in *PITX2* by other researchers [6,40]. Recurrent spontaneous miscarriages have not previously been reported in individuals with mutations in *PITX2*. It is as yet not possible to determine whether these unusual symptoms are associated with ARS, or perhaps caused by other underlying factors.

In summary, the clinical features of the affected individuals in a four-generation Chinese family with ARS were reported. A 53,840 bp genomic deletion spanning *PITX2* and *PANCR* was identified to be responsible for the disease in this particular family. This study widens our understanding of the phenotypic and mutational spectrum of *PITX2*-associated Axenfeld-Rieger syndrome. This work suggests that patients with mutations in *PITX2*, even with no signs of heart problems, should undergo an ECG to assess the risk of heart dysfunction and arrhythmias.

#### APPENDIX 1. PRIMERS USED FOR MUTATION SCREENING IN *PITX2* AND *FOXC1*.

To access the data, click or select the words “[Appendix 1.](#)”

#### APPENDIX 2. PRIMERS USED FOR QPCR IN THE DETECTION OF *PITX2* DELETION.

To access the data, click or select the words “[Appendix 2.](#)”

#### APPENDIX 3. DATA SETS.

To access the data, click or select the words “[Appendix 3.](#)” Candidate variants on the X chromosome with a MAF under 0.005.

#### APPENDIX 4. CO-SEGREGATION ANALYSIS OF THE *PITX2* LARGE DELETION FOR ALL PARTICIPANTS IN THE FAMILY BY PCR USING THE -26.4K-F/+4.5K-R PRIMER PAIR.

To access the data, click or select the words “[Appendix 4.](#)”

## ACKNOWLEDGMENTS

The authors are grateful to the family members for participating in this study. We thank Dr. Min Ming and Dr. Jiangfeng Yuan (Yangxin People’s Hospital, Hubei, China) for their kind help in the clinical examinations of some family members. We also thank Dr Steven Patterson (Department of Biologic and Biomedical Sciences, Glasgow Caledonian University, Glasgow, Scotland) for English proofreading. This study was supported by grants from the National Natural Science Foundation of China (No.31601026, No.81670890, No.31801041, and No.31871260). To whom correspondence should be sent: Dr. Fei Liu ([liufei05@hust.edu.cn](mailto:liufei05@hust.edu.cn)) or Dr. Pengcheng Li ([lipengcheng72@126.com](mailto:lipengcheng72@126.com)).

## REFERENCES

- Seifi M, Walter MA. Axenfeld-Rieger syndrome. *Clin Genet* 2018; 93:1123-30. [PMID: 28972279].
- Chang TC, Summers CG, Schimmenti LA, Grajewski AL. Axenfeld-Rieger syndrome: new perspectives. *Br J Ophthalmol* 2012; 96:318-22. [PMID: 22199394].
- Hendee KE, Sorokina EA, Muheisen SS, Reis LM, Tyler RC, Markovic V, Cuturilo G, Link BA, Semina EV. *PITX2* deficiency and associated human disease: insights from the zebrafish model. *Hum Mol Genet* 2018; 27:1675-95. [PMID: 29506241].
- Tümer Z, Bach-Holm D. Axenfeld-Rieger syndrome and spectrum of *PITX2* and *FOXC1* mutations. *Eur J Hum Genet* 2009; 17:1527-39. [PMID: 19513095].
- D’haene B, Meire F, Claerhout I, Kroes HY, Plomp A, Arens YH, de Ravel T, Casteels I, De Jaegere S, Hooghe S, Wuyts W, van den Ende J, Roulez F, Veenstra-Knol HE, Oldenburg RA, Giltay J, Verheij JB, de Faber JT, Menten B, De Paepe A, Kestelyn P, Leroy BP, De Baere E. Expanding the spectrum of *FOXC1* and *PITX2* mutations and copy number changes in patients with anterior segment malformations. *Invest Ophthalmol Vis Sci* 2011; 52:324-33. [PMID: 20881294].
- Reis LM, Tyler RC, Volkmann Kloss BA, Schilter KF, Levin AV, Lowry RB, Zwijnenburg PJ, Stroh E, Broeckel U, Murray JC, Semina EV. *PITX2* and *FOXC1* spectrum of mutations in ocular syndromes. *Eur J Hum Genet* 2012; 20:1224-33. [PMID: 22569110].
- Protas ME, Weh E, Footz T, Kasberger J, Baraban SC, Levin AV, Katz LJ, Ritch R, Walter MA, Semina EV, Gould DB. Mutations of conserved non-coding elements of *PITX2* in patients with ocular dysgenesis and developmental glaucoma. *Hum Mol Genet* 2017; 26:3630-8. [PMID: 28911203].
- Tanwar M, Dada T, Dada R. Axenfeld-Rieger Syndrome Associated with Congenital Glaucoma and Cytochrome P4501B1 Gene Mutations. *Case Rep Med* 2010; 2010:212656-[PMID: 20827438].
- Micheal S, Siddiqui SN, Zafar SN, Venselaar H, Qamar R, Khan MI, den Hollander AI. Whole exome sequencing

- identifies a heterozygous missense variant in the PRDM5 gene in a family with Axenfeld-Rieger syndrome. *Neurogenetics* 2016; 17:17-23. [PMID: 26489929].
10. Phillips JC, del Bono EA, Haines JL, Pralea AM, Cohen JS, Greff LJ, Wiggs JL. A second locus for Rieger syndrome maps to chromosome 13q14. *Am J Hum Genet* 1996; 59:613-9. [PMID: 8751862].
  11. Strungaru MH, Dinu I, Walter MA. Genotype-phenotype correlations in Axenfeld-Rieger malformation and glaucoma patients with FOXC1 and PITX2 mutations. *Invest Ophthalmol Vis Sci* 2007; 48:228-37. [PMID: 17197537].
  12. Intarak N, Theerapanon T, Ittiwut C, Suphapeetiporn K, Porn-taveetus T, Shotelersuk V. A novel PITX2 mutation in non-syndromic orodental anomalies. *Oral Dis* 2018; 24:611-8. [PMID: 29121437].
  13. Vande Perre P, Zazo Seco C, Patat O, Bouneau L, Vigouroux A, Bourgeois D, El Hout S, Chassaing N, Calvas P. 4q25 microdeletion encompassing PITX2: A patient presenting with tetralogy of Fallot and dental anomalies without ocular features. *Eur J Med Genet* 2018; 61:72-8. [PMID: 29100920].
  14. Mechakra A, Footz T, Walter M, Aranega A, Hernandez-Torres F, Morel E, Millat G, Yang YQ, Chahine M, Chevalier P, Christie G. A Novel PITX2c Gain-of-Function Mutation, p.Met207Val, in Patients With Familial Atrial Fibrillation. *Am J Cardiol* 2019; 123:787-93. [PMID: 30558760].
  15. Wei D, Gong XH, Qiu G, Wang J, Yang YQ. Novel PITX2c loss-of-function mutations associated with complex congenital heart disease. *Int J Mol Med* 2014; 33:1201-8. [PMID: 24604414].
  16. Wang J, Zhang DF, Sun YM, Yang YQ. A novel PITX2c loss-of-function mutation associated with familial atrial fibrillation. *Eur J Med Genet* 2014; 57:25-31. [PMID: 24333117].
  17. Liu F, Li P, Liu Y, Li W, Wong F, Du R, Wang L, Li C, Jiang F, Tang Z, Liu M. Novel compound heterozygous mutations in MYO7A in a Chinese family with Usher syndrome type 1. *Mol Vis* 2013; 19:695-701. [PMID: 23559863].
  18. Tang Z, Wang Z, Wang Z, Ke T, Wang QK, Liu M. Novel compound heterozygous mutations in CERKL cause autosomal recessive retinitis pigmentosa in a nonconsanguineous Chinese family. *Arch Ophthalmol* 2009; 127:1077-8. [PMID: 19667359].
  19. Zhang S, Wang L, Hao Y, Wang P, Hao P, Yin K, Wang QK, Liu M. T14484C and T14502C in the mitochondrial ND6 gene are associated with Leber's hereditary optic neuropathy in a Chinese family. *Mitochondrion* 2008; 8:205-10. [PMID: 18440284].
  20. Gao M, Zhang S, Liu C, Qin Y, Archacki S, Jin L, Wang Y, Liu F, Chen J, Liu Y, Wang J, Huang M, Liao S, Tang Z, Guo AY, Jiang F, Liu M. Whole exome sequencing identifies a novel NRL mutation in a Chinese family with autosomal dominant retinitis pigmentosa. *Mol Vis* 2016; 22:234-42. [PMID: 27081294].
  21. Li H, Durbin R. Fast and accurate long-read alignment with Burrows-Wheeler transform. *Bioinformatics* 2010; 26:589-95. [PMID: 20080505].
  22. Van der Auwera GA, Carneiro MO, Hartl C, Poplin R, Del Angel G, Levy-Moonshine A, Jordan T, Shakir K, Roazen D, Thibault J, Banks E, Garimella KV, Altshuler D, Gabriel S, DePristo MA. From FastQ data to high confidence variant calls: the Genome Analysis Toolkit best practices pipeline. *Curr Protoc Bioinformatics* 2013; 43:11-[PMID: 25431634].
  23. Yang H, Wang K. Genomic variant annotation and prioritization with ANNOVAR and wANNOVAR. *Nat Protoc* 2015; 10:1556-66. [PMID: 26379229].
  24. Yunliang S, Yuqiang H, Ying-Peng L, Ming-Zhi Z, Lam DS, Rao SK. Corneal endothelial cell density and morphology in healthy Chinese eyes. *Cornea* 2007; 26:130-2. [PMID: 17251798].
  25. Nadadur RD, Broman MT, Boukens B, Mazurek SR, Yang X, van den Boogaard M, Bekeny J, Gadek M, Ward T, Zhang M, Qiao Y, Martin JF, Seidman CE, Seidman J, Christofels V, Efimov IR, McNally EM, Weber CR, Moskowitz IP. Pitx2 modulates a Tbx5-dependent gene regulatory network to maintain atrial rhythm. *Sci Transl Med* 2016; 8:354ra115-[PMID: 27582060].
  26. Kirchhof P, Kahr PC, Kaese S, Piccini I, Vokshi I, Scheld HH, Rotering H, Fortmueller L, Laakmann S, Verheule S, Schotten U, Fabritz L, Brown NA. PITX2c is expressed in the adult left atrium, and reducing Pitx2c expression promotes atrial fibrillation inducibility and complex changes in gene expression. *Circ Cardiovasc Genet* 2011; 4:123-33. [PMID: 21282332].
  27. Chinchilla A, Daimi H, Lozano-Velasco E, Dominguez JN, Caballero R, Delpon E, Tamargo J, Cinca J, Hove-Madsen L, Aranega AE, Franco D. PITX2 insufficiency leads to atrial electrical and structural remodeling linked to arrhythmogenesis. *Circ Cardiovasc Genet* 2011; 4:269-79. [PMID: 21511879].
  28. Wang J, Klysis E, Sood S, Johnson RL, Wehrens XH, Martin JF. Pitx2 prevents susceptibility to atrial arrhythmias by inhibiting left-sided pacemaker specification. *Proc Natl Acad Sci USA* 2010; 107:9753-8. [PMID: 20457925].
  29. Gore-Panter SR, Hsu J, Barnard J, Moravec CS, Van Wagoner DR, Chung MK, Smith JD. PANCR, the PITX2 Adjacent Noncoding RNA, Is Expressed in Human Left Atria and Regulates PITX2c Expression. *Circ Arrhythm Electrophysiol* 2016; 9:e003197-[PMID: 26783232].
  30. Sun YM, Wang J, Qiu XB, Yuan F, Xu YJ, Li RG, Qu XK, Huang RT, Xue S, Yang YQ. PITX2 loss-of-function mutation contributes to tetralogy of Fallot. *Gene* 2016; 577:258-64. [PMID: 26657035].
  31. Yuan F, Zhao L, Wang J, Zhang W, Li X, Qiu XB, Li RG, Xu YJ, Xu L, Qu XK, Fang WY, Yang YQ. PITX2c loss-of-function mutations responsible for congenital atrial septal defects. *Int J Med Sci* 2013; 10:1422-9. [PMID: 23983605].



32. Franco D, Sedmera D, Lozano-Velasco E. Multiple Roles of Pitx2 in Cardiac Development and Disease. *J Cardiovasc Dev Dis.* 2017; 4.
33. Waite MR, Martin DM. Axial level-specific regulation of neuronal development: lessons from PITX2. *J Neurosci Res* 2015; 93:195-8. [PMID: 25124216].
34. Hernandez-Torres F, Rodriguez-Outeirino L, Franco D, Aranega AE. Pitx2 in Embryonic and Adult Myogenesis. *Front Cell Dev Biol* 2017; 5:46-[PMID: 28507987].
35. Lin CR, Kioussi C, O'Connell S, Briata P, Szeto D, Liu F, Izpisua-Belmonte JC, Rosenfeld MG. Pitx2 regulates lung asymmetry, cardiac positioning and pituitary and tooth morphogenesis. *Nature* 1999; 401:279-82. [PMID: 10499586].
36. Lu MF, Pressman C, Dyer R, Johnson RL, Martin JF. Function of Rieger syndrome gene in left-right asymmetry and craniofacial development. *Nature* 1999; 401:276-8. [PMID: 10499585].
37. Chen L, Gage PJ. Heterozygous Pitx2 Null Mice Accurately Recapitulate the Ocular Features of Axenfeld-Rieger Syndrome and Congenital Glaucoma. *Invest Ophthalmol Vis Sci* 2016; 57:5023-30. [PMID: 27654429].
38. Pappone C, Vicedomini G, Manguso F, Saviano M, Baldi M, Pappone A, Ciaccio C, Giannelli L, Ionescu B, Petretta A, Vitale R, Cuko A, Calovic Z, Fundaliotis A, Moscatiello M, Tavazzi L, Santinelli V. Wolff-Parkinson-White syndrome in the era of catheter ablation: insights from a registry study of 2169 patients. *Circulation* 2014; 130:811-9. [PMID: 25052405].
39. Diehl AG, Zareparsis S, Qian M, Khanna R, Angeles R, Gage PJ. Extraocular muscle morphogenesis and gene expression are regulated by Pitx2 gene dose. *Invest Ophthalmol Vis Sci* 2006; 47:1785-93. [PMID: 16638982].
40. Titheradge H, Togneri F, McMullan D, Brueton L, Lim D, Williams D. Axenfeld-Rieger syndrome: further clinical and array delineation of four unrelated patients with a 4q25 microdeletion. *Am J Med Genet A* 2014; 164A:1695-701. [PMID: 24715413].

Articles are provided courtesy of Emory University and the Zhongshan Ophthalmic Center, Sun Yat-sen University, P.R. China. The print version of this article was created on 4 October 2020. This reflects all typographical corrections and errata to the article through that date. Details of any changes may be found in the online version of the article.